MULTIWAVELENGTH OBSERVATIONS OF γ-RAY BURSTS DETECTED BY INTEGRAL

A. J. Castro-Tirado[1], J. Gorosabel[1], A. de Ugarte Postigo[1], M. Jelínek[1], V. Reglero[2], P. Kubánek[2], L. Sabau-Graziati[3], and S. Guziy[4]

[1]*Instituto de Astrofísica de Andalucía (IAA-CSIC), P.O. Box 03004, E-18080 Granada, Spain*
[2]*Grupo de Astronomía y Ciencias del Espacio, Universidad de Valencia, 46071 Burjassot (Valencia), Spain*
[3]*Instituto Nacional de Técnica Aerospacial (INTA), 28850 Torrejón de Ardoz (Madrid), Spain*
[4]*Nikolaev State University, Nikolskaya 24, 54030 Nikolaev, Ukraine*

ABSTRACT

We present an overview of GRBs detected by *INTEGRAL* for the period Nov 2002-Sep 2006. 40 events have been imaged so far by IBIS/ISGRI (implying a detection rate of ~ 0.9 month^{-1}). The fact that a significant fraction of the *INTEGRAL* pointings are devoted to the Galactic Plane, makes many GRB afterglows elusive at optical wavelengths due to a considerable extinction in the line of sight. In any case, only five events can be considered as having bright optical/near-IR afterglows (after correcting for Galactic extinction), where the remaining ones have faint counterparts (being either intrinsically faint or lying at redshifts $z > 3$) or are really truly dark events (also possible due to very high extinction in their host galaxies).

Key words: gamma-ray bursts; multiwavelength observations.

1. INTRODUCTION

A significant fraction of γ-ray bursts (GRBs) seem to be intrinsically faint. However the fact that they could be intrinsically dark events remains an open question (see [1] and references therein). In some cases, it has been suggested that the cause of the reddening is dust extinction in the host galaxy. On the other hand, ultra-high redshift events appear quite faint because of Lyman-α blanketing affecting the optical passbands.

With the launch of *Swift* in Nov 2004, which has the capability to follow-up the events detected by the GRB detector onboard (BAT) or by other satellites like *HETE-2* and *INTEGRAL*, it is possible to zoom in on this population of optically faint events in order to disentangle their nature.

Here we present an overview of GRBs detected by *INTEGRAL*. The corresponding detection rates of the different *INTEGRAL* instruments are SPI/ACS: ~ 0.5 day^{-1} (but no position derived), IBIS/ISGRI: ~ 0.8 month^{-1}, JEM-X: ~ 0.5 yr^{-1}, OMC: ~ 0.2 yr^{-1}. Alerts transmitted in near-real time to ground thanks to IBAS software [2] (positions accurate to 3′ 90% confidence level), make possible the detection of afterglows for some bursts in all wavelengths, from X-rays to radio.

Up to now, 40 events have been detected by IBIS/ISGRI so far, with GRB 021125 (Fig. 1) being the first one to be imaged [3]. Out of them, 37 can be considered as classical long GRBs while 3 have properties reminiscent of X-ray flashes (XRFs). X-ray afterglows (XRAs) have been observed for 13 of them. Optical afterglows (OAs) have been observed for another 12 OAs, with only two radio afterglows being detected so far. The number of firmly established redshifts from optical absorption line spectroscopy is 4 (with another tentative 3 redshifts that cannot be confirmed for the time being).

2. SEARCHES FOR SIMULTANEOUS PROMPT EMISSION

Searches for simultaneous prompt emission have been performed for three GRBs: GRB 041219, GRB 050502A and GRB 050504. Upper limits were imposed for both GRB 050502A (observed at BOOTES-2, R $\geq$ 8.5 [4]) and GRB 050504 (observed by Ashra, R $\geq$ 8.0 [5]).

For GRB 041219A, the contemporaneous emission was detected in both the optical [6] and the near-infrared (nIR) [7]. Prompt optical emission from GRB 041219A was seen to vary and correlate with the prompt γ-rays (Fig. 2), indicating a common origin for the optical light and the γ-rays. Within the context of the standard fireball model of GRBs, internal shocks driven into the burst ejecta by variations of the inner engine have been proposed as the origin of this prompt emission [6]. The initial infrared pulse suggests an origin consistent with internal shocks [7].

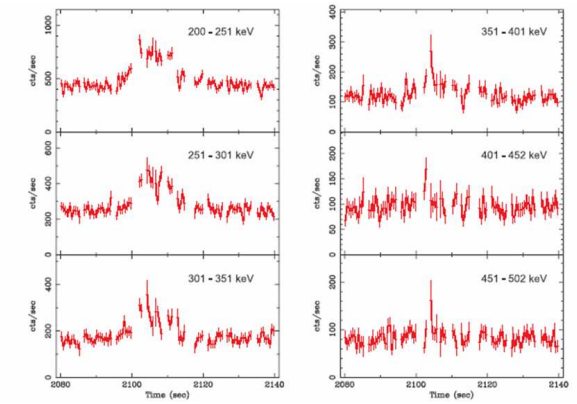

Figure 1. IBIS/PICsIT lightcurve of GRB 021125 in different energy bands. The time of the onset of the event was T_0 = 17:58:30 UT on 25 Nov 2002. From [3].

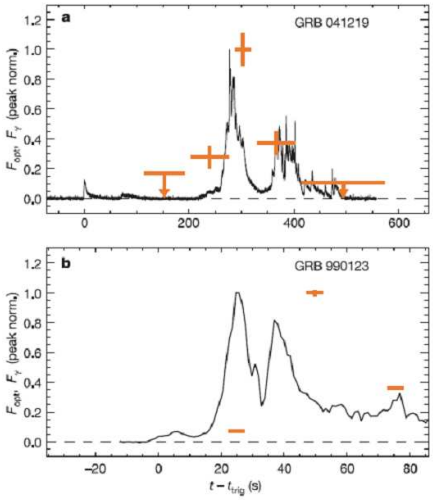

Figure 2. Comparison of the prompt γ-ray photons and prompt optical light, for both GRB 041219A and GRB 990123. From [6].

3. DETECTION OF AFTERGLOWS FROM X-RAYS TO RADIO

The importance of performing X-ray/optical/nIR/mm/radio follow-ups is understood in the context of determining the physical parameters of the afterglow and the prompt emission. Thus, the purpose is multifold:

- X-rays observations provide an accurate position (most essential in case of dark events) as well as valuable spectral and lightcurve information.
- Optical and nIR photometry is important in order to properly model the (usually) complex lightcurves and are most essential in case of very extincted objects and high redshift events.
- Prompt optical spectroscopy allow to determine z (and the burst energetics) and studying intervening systems in the line of sight.
- Polarimetric optical observations are difficult to perform but help in constraining the burst geometry and test the different theoretical models.
- Multiwavelength data (from X-ray to radio) are most essential for obtaining a proper modelling and determine the microphysics parameters of the shock.

3.1. Faint optical afterglows [R (dereddened) $>$ 21 at T_0 + 12 hr)]

Most *INTEGRAL* GRB afterglows are faint or obscured at optical wavelengths. GRB 030131, GRB 030227, GRB 040106, GRB 040827, GRB 041218 and GRB 051211B are the six events that can be considered as belonging to the faint optical afterglow population.

GRB 030131: The position was promptly reported [8], with a faint optical afterglow (OA) being identified with R = 21 at T_0 + 3.2 hr [9], fading to R = 25 at T_0 + 29 hr [10].

GRB 030227: The first *INTEGRAL* GRB for which afterglow emission at other wavelengths than optical (ranging from X-ray to nIR) was reported [11]. The dim OA would not have been detected by many previous searches due to its faintess (R $\sim$ 23). It was seen to decline following a power law decay with index $\alpha = -0.95$. The spectral index $\beta_{opt/nIR}$ yielded -1.25 ± 0.14, values that may be explained by a relativistic expansion of a fireball (with p = 2.0) in the fast cooling regime. It was also followed-up by *XMM-Newton* follow-up at T_0 + 8 hr. The EPIC-pn spectrum revealed no emission line features [12]. However, other authors [13] made use of the RGS spectral data from which a set of spectral features could be associated with emission lines at z = 1.4 (Fig. 3). The strong delayed X-ray line emission was detected in the X-ray afterglow, appearing near the end of the *XMM-Newton* observation, nearly 20 hr after the burst. The lines correspond to H- and/or He-like emission from Mg, Si, S, Ar and Ca at the above mentioned redshift. An inverse Compton contribution (Fig. 4) was also invoked in order to explain the high spectral flux that was observed [11].

GRB 040106: The OA was detected with R = 22.4 at T_0 + 16 hr and R = 23.7 at 40 hr at the VLT [14]. A *XMM-Newton* ToO was performed at T_0 + 6 hr. From the X-ray spectral index and temporal decay, it was argued that the afterglow was consistent with a fireball expanding in a wind environment. A constant density environment was

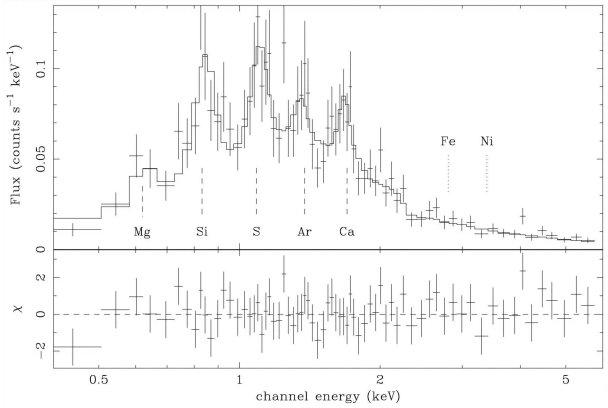

Figure 3. EPIC-pn spectrum for the last 11 ksec of the GRB 030227 X-ray afterglow observation. The Kα lines of H-like Mg, Si, S, Ar and Ca (redshifted by z = 1.39) are marked with dotted lines. From [13].

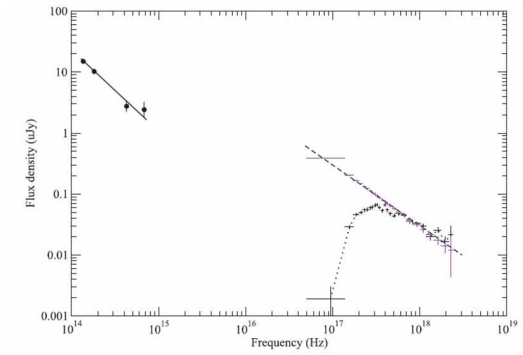

Figure 4. The broad-band spectrum for the GRB 030227 afterglow at T_0 + 0.87 d. Inverse Compton contribution is needed to explain the high flux observed at X-rays. From [11].

excluded by the data [15].

GRB 040827: Followed up by MASTER at T_0 + 7 min, neither optical [16] nor radio afterglow were detected [17]. A *XMM-Newton* observation starting at T_0 + 6 hr led to the detection of a fading X-ray afterglow with the X-ray flux following $F \propto t^{-1.4}$. The spectrum is well described by a power law (Γ = 2.3) affected by an absorption column largely exceeding (by a factor 5) the expected Galactic one, requiring the contribution of an intrinsic, redshifted absorber [18]. In the optical/nIR range, the afterglow emission was observed in the K-band [18,19] superimposed to the host galaxy; with the flux in other bands being dominated by the host galaxy (K = 19.5). A gas column density in the range N(H) = (0.4 - 2.6) $\times$ 10^{21} cm^{-2}, likely located at a redshift $0.5 < z < 1.7$. According to [18], GRB 040827 is, amongst all *INTEGRAL* events detected so far, the best example of an X-ray afterglow with intrinsic absorption.

GRB 041218: The OA was reported at Calar Alto [20]. A tentative redshift of z = 0.8 has been proposed on the basis of a single absorption-line identification [21].

GRB 051211B: A *Swift/XRT* ToO started at T_0 + 3 hr, allowing to detect the X-ray afterglow [22]. Within the tiny X-ray error box, a radio transient was also detected [23]. The OA was recorded in the early I-band frames obtained at the 1.5m telescope in Sierra Nevada [24]. See [25] for additional details.

3.2. Bright optical afterglows [R (dereddened) $<$ 21 at T_0 + 12 hr] and the low b^{II} bright OA population

Only six events detected by *INTEGRAL* can be considered as part of the bright OA population: GRB 031203, GRB 041219A, GRB 040422, GRB 050502A, GRB 050525A and GRB 060912B.

GRB 031203: At low Galactic latitudes (b^{II}), this was the first GRB for which a time-dependent dust scattered X-ray halo was detected (Fig. 5). The X-ray afterglow was observed by *XMM-Newton* starting 6 hr after the burst. The halo appeared as concentric ringlike structures centered on the GRB location. The radii of these structures increased with time as $t^{1/2}$, consistent with small-angle X-ray scattering caused by a large column of dust along the line of sight. The rings are due to dust concentrated in two distinct slabs in our Galaxy located at distances of 880 and 1390 pc, consistent with known Galactic features. The halo brightness implies an initial soft X-ray pulse consistent with the observed GRB [26]. It was also proposed as an underluminous event ($E < 10^{50}$ erg) at z = 0.106 [27], making of GRB 031203 one of the nearest GRBs detected so far. Some other authors [28] argue that a 2nd soft pulse should have been produced. The difference between the soft and hard X-ray spectra from *XMM-Newton* and *INTEGRAL* indicates that a second soft pulse probably occurred in this burst, as has been observed in other GRBs, notably GRB 050502B. An underlying supernova, dubbed SN 2003lw [29-31] emerged few days after the onset of the event. In fact, a very faint afterglow is detected superposed onto the host galaxy in the initial nIR observations, carried out $\sim$ 9 hr after the burst. Subsequently, a rebrightening was detected in all bands, peaking in the R band about 18 rest-frame days after the burst. In fact, spectra taken close to the maximum of the rebrightening show extremely broad features as in SN 1998bw, with an estimaded absolute magnitude M_V = -19.75 ± 0.15 [29]. However, the J-band lightcurve differs significantly from that of SN 1998bw if both were occurring at the same redshift [30]. It has been also considered as an analogue to GRB 980425 / SN 1998bw (Fig. 6). In fact, radio and X-ray afterglow observations reveal that it is sub-energetic which, when taken together with the low gamma-ray luminosity, suggests that GRB 031203 is the first cosmic analogue to GRB 980425 [32]. It has been modelled as an event in which a highly colli-

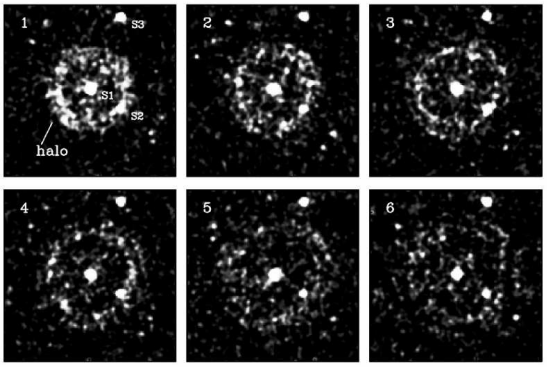

Figure 5. The GRB 031203 X-ray dust-scattered halo as observed by XMM-Newton. From [26].

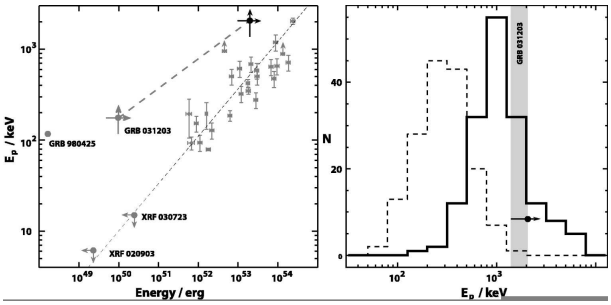

Figure 6. The location of GRB 031203 in the E_p - E_γ plane. From [33] and references therein.

mated explosion was viewed off-axis [33]. In fact, there might be a large population of such events in the Universe that are difficult to detect due to the limited sensitivity of the current instruments aboad scientific spacecraft.

GRB 041219A: The brightest burst detected by *INTEGRAL* according to its gamma-ray fluence. Images started 8 minutes after the burst at the 2.2m Calar Alto telescope. A mm detection was obtained at PdB interferometer. A nIR flash was also recorded starting at T_0 + 7 min [7] and could be interpreted as re-radiation of dust in a circumstellar cloud [34]: the bolometric light curves for the afterglow resulting from the passage of the blast wave through a molecular cloud were computed, implying that the peak of the emission could be reached as soon as seven days (the gamma-ray burst is located at some distance from the center of a molecular cloud with small-scale density enhancements), or as long as one to three years (the gamma-ray burst is located at the center of a uniform molecular cloud) after the burst. The bolometric luminosity of the re-radiated signal can reach 6.5×10^{42} erg/s. See Fig. 7.

GRB 040422: At 3 degrees above the Galactic Plane, its nIR afterglow was detected. The IBIS spectrum is well fit by the Band model with a break energy of E_0= 56 keV

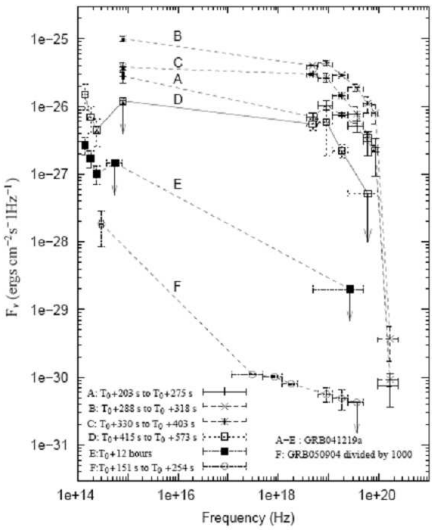

Figure 7. Broadband spectra of GRB 041219 and GRB 050904 (at z = 6.29) for comparison purposes. From [35].

and E_{peak} = 41 keV. The peak flux is 1.8×10^{-7} erg cm^{-2} s^{-1} and fluence 3.4×10^{-7} erg cm^{-2} in the range 20-200 keV. The afterglow was imaged less than 2 h after the burst, leading to the discovery of its near-infrared afterglow. No detection could have been obtained in the optical R and I bands, partly due to the large extinction in the Milky Way. It is one of the dimmest GRBs, which it is superimposed on a K = 20.3 host galaxy. A comparison of the magnitude of the afterglow with those of a compilation of promptly observed counterparts of previous GRBs, reeals that the afterglow of GRB 040422 lies at the very faint end of the distribution, only brighter than that of GRB 021211, singled out later and in the optical bands, and GRB 040924 after accounting for Milky Way extinction [36].

GRB 050502A: The brightest OA (R = 14.3) of all events detected by *INTEGRAL* with an early optical (unfiltred) detection (T_0 + 23.5 s) by ROTSE-III [37]. The nIR afterglow was registered at T_0 + 31 min [38]. z = 3.793 was derived from Keck spectroscopy [39]. The light curve in the optical band can be described by a simple power law with index of 1.2 $\pm$ 0.1, with evidence for a bump rising at T_0 + 0.02 days, probably implying the existence of a uniform circumburst medium with clumps in density, as in the case of GRB 021004 [40]. See Fig. 8.

GRB 050525A: It was detected by *Swift* but was also observed at the edge of the IBIS field of view. Early optical detection was recorded by BOOTES and *Swift*/UVOT. The X-ray afterglow was well monitored by *Swift*/XRT [41] with a reported jet-break at 0.15 days and z = 0.606 was determined from absorption spectroscopy. It provided unique multiwavelength coverage from the very earliest phases of the burst. The X-ray and optical/UV afterglow decay light curves both exhibit a steeper slope $\sim$ 0.15 days after the burst, indicative of a jet break. This jet

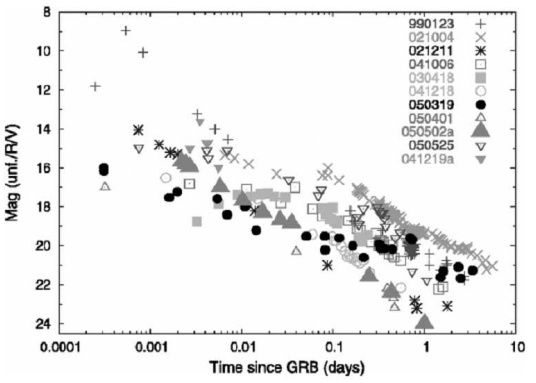

Figure 8. Early lightcurves for a set of GRBs with optical detections the minutes after the burst onset, including the INTEGRAL GRB 041219A, GRB 050502A and GRB 050525A. From [40].

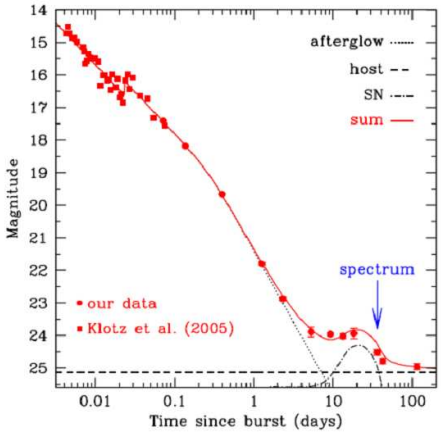

Figure 9. Optical lightcurve of the GRB 050525A afterflow. The dotted, dashed, and dot-dashed lines indicate the afterglow, the host galaxy, and the supernova contributions, respectively. The continuous, thick line is the sum of them all. The arrow points the time when an optical spectrum was gathered at the VLT. From [42].

break time combined with the total gamma-ray energy of the burst constrains the opening angle of the jet to be 3.2°. Prior to the jet break, the X-ray data can be modeled by a simple power law with index $\alpha = -1.2$. However, after 300 s the X-ray flux brightens by about 30% compared to the power-law fit. The optical/UV data have a more complex decay, with evidence of a rapidly falling reverse shock component that dominates in the first minute or so, giving way to a flatter forward shock component at later times. The multiwavelength X-ray/UV/optical spectrum of the afterglow showed evidence for migration of the electron cooling frequency through the optical range within 25,000 s. The measured temporal decay and spectral indexes in the X-ray and optical/UV regimes compare favorably with the standard fireball model for gamma-ray bursts assuming expansion into a constant-density interstellar medium. The early-time light curve is described by a broken power law with a break at t $\sim$ 0.3 days after the burst. About 5 days after the burst, a flattening is apparent, followed by further dimming. Both the magnitude and the shape of the light curve suggest that a supernova was emerging during the late decay of the afterglow (Fig. 9). This supernova, named SN 2005nc, had a rise time faster than SN 1998bw and a long-lasting maximum. A spectrum obtained about 20 days (rest frame) after the GRB resembles the spectrum of SN 1998bw obtained close to maximum light [42]. See Fig. 10.

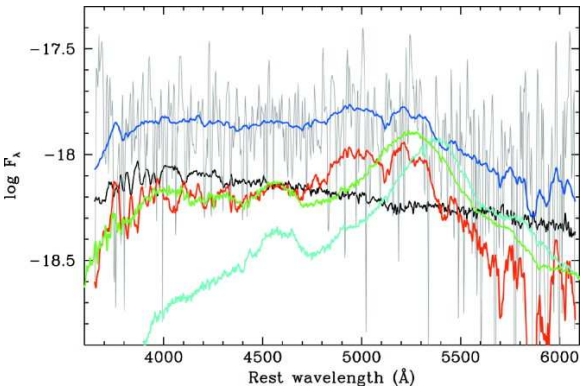

Figure 10. Optical spectrum at the time of the SN 2005nc / GRB 050525A maximum light. Also plotted, from the top to the bottom of the figure, are the rebinned spectrum, a template spectrum for a blue star-forming galaxy, the subtracted spectrum, the spectrum of SN 1998bw 5 days past maximum and the spectrum of SN 1998bw 10 days past maximum. From [42].

GRB 060912B: It was originally recorded by *Swift* detecting bright X-ray and optical (R $\sim$ 16.1) afterglows [43]. The redshift was estimated as $z = 0.937$ [44].

3.3. Dark events

Eight *INTEGRAL* events have been followed-up down to reasonable deep limits at optical/nIR wavelenghts but no

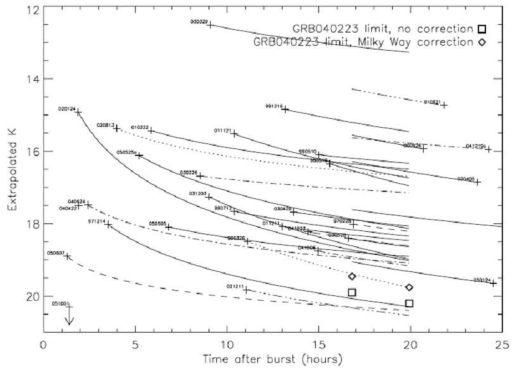

Figure 11. Near-IR lightcurves of several GRB afterglows, including GRB 040223. From [45].

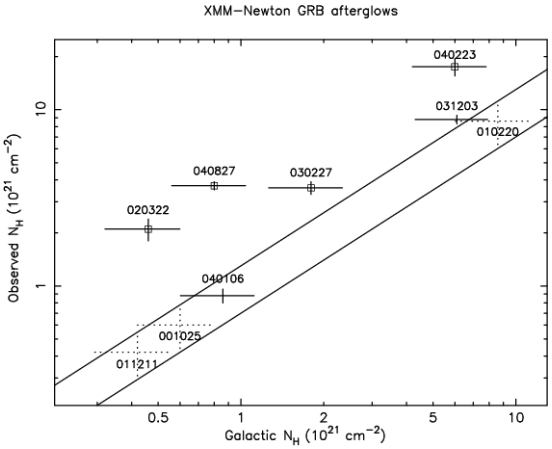

Figure 12. Summary of XMM-Newton results for derived intrisic absorption of GRB afterglows, including the INTEGRAL events GRB 030227, GRB 040223, GRB 040827 and GRB 041219A. Solid lines correspond to an $N_{\rm H}$ = Galactic $N_{\rm H} \pm 30\%$, which represent a reasonable guess of the uncertainty affecting Galactic column density estimates. Adapted from [18].

afterglows could be found. These are GRB 040223, GRB 040812, GRB 050504, GRB 050520, GRB 050522, GRB 050714A, GRB 060901 and GRB 060930. A more detailed information follows.

GRB 040223: A dark event similar to GRB 040624, among the weakest and longest bursts detected by *INTEGRAL*. A *XMM-Newton* observation was performed at T_0 + 5 hr, from which a extremely high column density N(H) = 1.6×10^{22} cm^{-2} was derived with a redshift $z < 1.7$ if N(H) (local) = 10^{22} cm^{-2} or $z > 7$ if due to Fe edge. A limit of K > 19.5 at T_0 + 17 hr [45] was derived in the nIR. See Fig. 11 and 12.

GRB 040812: *Chandra* observations started at T_0 + 5 d [46], finding no strong indication of a X-ray afterglow. No optical or radio counterparts were found either [47,48].

GRB 050504: The X-ray afterglow was detected by *Swift*/XRT on a follow-up observation at T_0 + 5.45 hr. A fading X-ray source was discovered with $(3.5 \pm 0.7) \times 10^{-3}$ cts/s. No optical afterglow was detected either, imposing limiting magnitudes of R > 16.0 at T_0 + 1 min [49], R > 21 at T_0 + 3 min [50]. The nIR afterglow was neither detected [51].

GRB 050520: The X-ray afterglow was detected by *Swift* at T_0 + 2 hr [52] with a countrate in the 0.5-10 keV band of $(2.8 \pm 0.5) \times 10^{-3}$ counts/s (implying an estimated unabsorbed 0.5-10 keV flux of 1.0×10^{-13} erg cm^{-2} s^{-1}). Limiting magnitudes on any optical afterglow were R > 16 at T_0 + 5 min [53] and I > 20 at To + 30 min [54]. The nIR afterglow was neither detected, implying K > 20 at T_0 + 6.5 hr [55]. Limits were imposed on the mm afterglow emission (F < 57 μJy) [56].

GRB 050522: The X-ray afterglow was detected by *Swift* at T_0 + 9 hr [57] with a count rate (0.5-10 keV) of $(1.6 \pm 0.5) \times 10^{-3}$ counts/s. Limiting magnitudes imposed on any optical afterglow were R > 18.7 at T_0 + 2 min [58]) No near-IR afterglow was found (K > 18.5) at T_0 + 2.3 hr [59]).

GRB 050714A: At low galactic latitude (8 degrees), the X-ray afterglow was detected by *Swift* at T_0 + 13.7 hr [60]. No OA was detected down to R > 18.2 at T_0 + 28 s [61]. There was a claim of a faint optical source within the XRT error box [62].

GRB 060901: An X-ray afterglow was detected by *Swift* although no optical or nIR counterparts were detected [63,64]. On the basis of its gamma-ray properties, a pseudo-$z = 2.0 \pm 0.5$ was estimated [65].

GRB 060930: An X-ray rich GRB with no optical or near-IR afterglows [66,67]. No follow-up X-ray observation by *Swift* was feasible.

4. INTEGRAL VS SWIFT GRB POPULATIONS

Since its launch in Nov 2004, *Swift* is recording ~ 100 bursts/yr. with $\sim$50% detected in optical, $\sim$30% in radio, and $\sim$15% in the nIR alone. The number of measured redshifts is $\sim$60, in the range 0.033-6.29 with $< z > = 2.7$

INTEGRAL is efficiently detecting and localizing long GRBs at a rate of 0.8 month^{-1}, but are *INTEGRAL* and *Swift* sampling the same population of GRBs ?

According to the results given in [68], taking into account the different efficiency of the two detectors (IBIS/ISGRI and BAT), about 10% of the events detected by *INTEGRAL* should be at a redshift larger than 5 (compared to 5% for the case of *Swift*).

Table 1. The list of the 40 INTEGRAL long-duration GRBs detected for the time interval Nov 2002 to Sep 2006. X-ray rich events are marked "X" following the usual naming convention YYMMDD.

021125	021219	030131	030227
030320	030501	030529	031203X
040106	040223	040323	040403
040422	040624	040730	040812
040827	040903X	041015	041218
041219A	050129	050223	050502A
050504	050520	050522X	050525A
050626	050714A	050918	050922A
051105B	051211B	060114	060130
060204A	060901	060912B	060930

5. CONCLUSIONS

INTEGRAL and *Swift* are providing a unique opportunity to unveil the remaining misteries in the GRB field in the coming years. 40 events have been detected so far by IBIS/ISGRI (implying a detection rate of ~ 0.9 month^{-1}). See Table 1. Good follow-up observations have been performed for $\sim$ 50% of *INTEGRAL* events, leading to the detection of 11 optical/nIR counterparts. 6 of them could be considered as belonging to the faint optical afterglow population, 6 could be representative of the bright optical afterglow population, and 8 could be considered as true dark events. In any case, the fact the a significant fraction of the *INTEGRAL* pointings are devoted to the Galactic Plane, makes that many events are elusive at optical wavelengths due to a considerable extinction in the line of sight.

Complementary observations in conjunction with other satellites and from ground-based observatories are most essential (i.e. follow-ups by *Swift* -7 XRAs so far- and *XMM-Newton* -5 XRAs so far-).

On the aggregate, the majority of afterglows are intrinsically faint or highly-reddened in the optical, thus preventing high-quality S/N spectra to determine a larger number of redshifts. The reason of the faintness is not well determined, but an origin at $z > 3$ for a significant fraction of the events seems plausible.

The lack of short-GRBs (< 3 %) detected by IBIS/ISGRI is unconsistent with the *Swift*/BAT detection rate of about 10% (compared to 25% in *CGRO*/BATSE). A possible reason might be a slightly different triggering criterium as the bandpass for IBIS/ISGRI and BAT (15-150 keV in imaging mode and extending up to 500 keV) are similar (both are based on CdZnTe detectors). In both IBIS/ISGRI and BAT, the burst trigger algorithm looks for excesses in the detector count rate above expected background and constant sources with images of the sky being produced as soon as a trigger is generated in order to check the reality of the trigger source. But probably the main difference will be the different field of view (5.5 times larger in BAT) besides the collecting area (2.0 times larger in BAT [69]) which results in BAT being more sensitive than IBIS for picking up the faint (and rare) short GRBs.

In any case, let us hope for a non-dark GRB at moderate or high b^{II} within the OMC FOV during the *INTEGRAL* mission lifetime !

ACKNOWLEDGEMENTS

We thank fruitful discussions with N. Lund, S. Brandt, M. Bremer, R. Hudec and V. V. Sokolov. We acknowledge S. Mereghetti and D. Götz for implementing the IBAS GRB alert software at an early stage of the mission. We also thanks S. Barthelmy for his work in BACODINE allowing to diseminate the *INTEGRAL* alerts in real time.

REFERENCES

[1] Castro-Tirado, A. J. et al. 2006, A&A 459, 763.
[2] Mereghetti, S. et al. 2003, A&A 411, L291.
[3] Malaguti, G. et al. 2003, A&A 411, 307.
[4] Jelínek, M. et al. 2007, in preparation.
[5] Sasaki, M. et al. 2005, GCNC 3499.
[6] Vestrand, W. T. et al. 2005, Nat 435, 178.
[7] Blake, C. H. et al. 2005, Nat 435, 181.
[8] Gotz, D. et al. 2003, A&A 409, 831.
[9] Fox, D. W. et al. 2003, GCNC 1857.
[10] Gorosabel, J. et al. 2003, GCNC 1866.
[11] Castro-Tirado, A. J. et al. 2003, A&A 411, L315.
[12] Mereghetti, S. et al. 2003, ApJ 590, L73.
[13] Watson, D. et al. 2003, ApJ 595, L29.
[14] Masetti, N. et al. 2004, GCNC 2515.
[15] Gendre, B. et al. 2004, A&A 424, L27.
[16] Lipunov, V. et al. 2004, GCNC 2676.
[17] Soderberg, A. & Frail, D. 2004, GCNC 2689.
[18] de Luca, A. et al. 2005, A&A 440, 85.
[19] Gladders, M. & Berger, E. 2004, GCNC 2681.
[20] Gorosabel, J. et al. 2004, GCNC 2861.
[21] de Ugarte Postigo, A. et al. 2007, in preparation.
[22] La Parola, V. et al. 2005, GCNC 4338.
[23] Frail, D. 2005, GCNC 4350.
[24] Jelínek, M. et al. 2005, GCNC 4358.
[25] McBreen, S. et al. 2007, in preparation.
[26] Vaughan, S. et al. 2004, ApJ 603, L5.
[27] Sazonov, S. et al. 2004, Nat 430, 646.

[28] Watson, D. et al. 2006, ApJ 636, 967.
[29] Malesani, D. et al. 2004, ApJ 609, L5.
[30] Gal-Yam, A. et al. 2004, ApJ 609, L59.
[31] Thomsen, B. et al. 2004, A&A 419, L21.
[32] Soderberg, A. et al. 2004, Nat 430, 648
[33] Ramírez-Ruiz, E. et al. 2004, ApJ 625, L91.
[34] Barkov, M. V. & Bisnovatiy-Kogan, G. S. 2005, Ap 48, 369.
[35] McBreen, S. et al. 2006, A&A 455, 433.
[36] Filliatre, P. et al. 2005, A&A 438, 793.
[37] Yost, S. A. et al. 2005, GCNC 3322.
[51] Bloom, J. S. & Blake, C. 2005, GCNC 3326.
[39] Prochaska, J. X. et al. 2005, GCNC 3332.
[40] Guidorzi, C. et al. 2005, ApJ 630, L121.
[41] Blustin, A. J. et al. 2006, ApJ 637, 901.
[42] Della Valle, M. et al. 2006, ApJ 642, L103.
[43] Hurkett, C. P. et al. 2006, GCNC 5558.
[44] Jakobsson, P. et al. 2006, GCNC 5617.
[45] Filliatre, P. et al. 2006, A&A 448, 971.
[46] Patel, S. et al. 2004, GCNC 2648.
[47] Berger, E. 2004, GCNC 2650.
[48] Kulkarni, S. R. et al. 2004, GCNC 2824.
[49] Sasaki, M. et al. 2005, GCNC 3421.
[50] Bradley Cenko, S. & Fox, D. E. 2005, GCNC 3349.
[51] Bloom, J. S. & Prochaska, J. X. 2005, GCNC 3347.
[52] Kennea, J. A. et al. 2005, GCNC 3434.
[53] Guidorzi, C. et al. 2005, GCNC 3437.
[54] de Ugarte Postigo, A. et al. 2005, GCNC 3432.
[55] Bradley Cenko, S. et al. 2005, GCNC 3438.
[56] Cameron, P. B. & Soderberg, A. M. 2005, GCNC 3453.
[57] Capalbi, M. et al. 2005, GCNC 3463.
[58] Li, W. 2005, GCNC 3447.
[59] Fox, D. W. et al. 2005, GCNC 3448.
[60] Racusin, J. L. et al. 2005, GCNC 3557.
[61] Schaefer, B. E. et al. 2005, GCNC 3608.
[62] Klose, S. et al. 2005, GCNC 3611.
[63] Cobb, B. E. et al. 2006, GCNC 5497.
[64] Wiersema, K. et al. 2006, GCNC 5501.
[65] Pelangeon, A. & Atteia, J. L. 2006, GCNC 5499.
[66] Swan, H. et al. 2006, GCNC 5666.
[67] de Ugarte Postigo, A. et al. 2006, GCNC 5701.
[68] Gorosabel, J. et al. 2004, A&A 427, 87.
[69] Barthelmy, S. D. et al. 2000, SPIE, vol 4140, 50.